Advances in Applied Mathematics and Mechanics
Adv. Appl. Math. Mech., Vol. **2**, No. 2, pp. 238-258

DOI: 10.4208/aamm.09-m0945
April 2010

Mathematical Modelling and Analysis of Lamb Waves in Elasto-Thermodiffusive Plates

J. N. Sharma[1,*] and P. K. Sharma[2]

[1] *Department of Applied Sciences, National Institute of Technology, Hamirpur 177 005, India*

[2] *Department of Mathematics, SL Bawa Dayanand Anglo Vedic College, Batala 143505, India*

Received 22 May 2009; Accepted (in revised version) 02 September 2009
Available online 5 March 2010

Abstract. The propagation characteristics of elasto-thermodiffusive Lamb waves in a homogenous isotropic, thermodiffusive, elastic plate have been investigated in the context of linear theory of generalized thermodiffusion. After developing the formal solution of the mathematical model consisting of partial differential equations, the secular equations have been derived by using relevant boundary conditions prevailing at the surfaces of the plate for symmetric and asymmetric wave modes in completely separate terms. The secular equations for long wavelength and short wavelength waves have also been deduced and discussed. The amplitudes of displacement components, temperature change and mass concentration under the Lamb wave propagation conditions have also been obtained. The complex transcendental secular equations have been solved by using a hybrid numerical technique consisting of irreducible Cardano method along with function iteration technique after splitting these in a system of real transcendental equations. The numerically simulated results in respect of phase velocity, attenuation coefficient, specific loss factor and relative frequency shift of thermoelastic diffusive waves have been presented graphically in the case of brass material.

AMS subject classifications: 74G15

Key words: Diffusion, Cardano method, relative frequency, thermal relaxation, iteration method.

1 Introduction

The use of Lamb waves for non-destructive evaluation of plates has attracted attention due to its interrogating efficiency over a reasonably extensive region. The influences of harmonically varying temperature and strain fields on the static and dynamic beha-

*Corresponding author.
Email: jns@recham.ernet.in (J. N. Sharma), pars1sharma70@yahoo.com (P. K. Sharma)

viour of plates have been investigated by Kozlov [1] and Massalas [2]. Saxena and Dhaliwal [3] studied two dimensional problems of axisymmetric and plane strain in coupled thermoelastic wave propagation in a homogenous isotropic plate. Kumar [4] investigated coupled thermoelastic waves in a plate of thickness $2h$ subjected to axially symmetric hydro-static tension by using integral transform technique. Sharma et al. [5] and Sharma [6] studied the propagation of thermoelastic waves in homogenous isotropic plates subjected to stress-free thermally insulated, stress-free isothermal, rigidly-fixed thermally insulated and rigidly-fixed isothermal boundary conditions in the context of generalized theories of thermoelasticity. Jin et al. [7] studied Lamb wave propagation and interaction in plates by using boundary element method.

The thermodiffusion in elastic solids occurs due to coupling of the fields of temperature, mass diffusion and strain fields in addition to heat and mass exchange with environment. Sherief et al. [8] derived the governing equations, variational principles and reciprocity theorems for generalized thermodiffusion in elastic solids in addition to the establishment of uniqueness of the solution under suitable conditions. Sherief and Saleh [9] studied the disturbance due to a time dependent thermal shock acting on the surface of a stress-free half-space with the help of Laplace transforms in the context of theory of generalized thermoelastic diffusion. Recently Aouadi [10] studied the elasto-thermodiffusive interactions in an infinitely long cylinder subjected to thermal shock on its surface with a permeating substance. Aouadi [11] used Laplace transform technique to investigate the problem of a stress free half-space whose surface is subjected to a time dependent thermal shock with variable electrical and thermal conductivity in the context of theory of generalized thermoelastic diffusion. Sharma [12] studied the propagation of plane harmonic generalized thermoelastic diffusive waves in heat conducting solids. It is found that there are three longitudinal waves, namely, elastodiffusive (ED), mass diffusion (MD-mode) and thermodiffusive (TD-mode) which are possible to propagate in such solids in addition to decoupled transverse waves. Sharma et al. [13] studied the problem of a stress free, homogenous isotropic, thermodiffusive elastic half space in the context of generalized theory of linear thermoelastic diffusion.

Keeping in view the applications of thermodiffusive processes, an attempt has been made in this paper to study various characteristics of elasto-thermodiffusive Lamb waves. The secular equations for plate waves have been obtained in the simplest form and closed mathematical conditions. The phase velocity, attenuation coefficient, specific loss factor of energy dissipation and relative frequency shift of wave propagation have been computed by using irreducible case of Cardano's method with the help of DeMoivre's theorem and functional iteration method from the transcendental secular equations. The computer simulation results have been presented graphically.

2 Formulation of the problem

We consider a homogenous isotropic, thermo diffusive elastic plate of thickness $2d$ in-

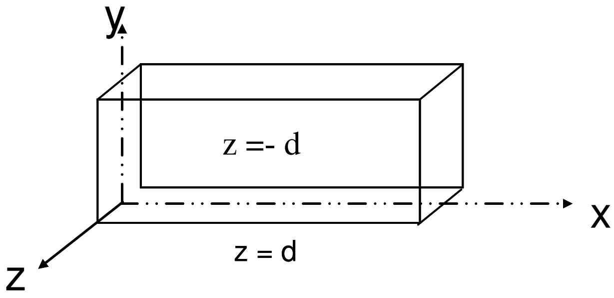

Figure 1: Geometry of the problem.

itially at uniform temperature T_0 and concentration C_0. We take origin of the rectangular Cartesian co-ordinate system $oxyz$ on the middle surface of the plate. The xy-plane is chosen to coincide with the middle surface of the plate and z-axis normal to it along the thickness. We take x-axis along the direction of wave propagation in such a way that all the particles on the line parallel to y-axis are equally displaced, so that all the field quantities are independent of y-co-ordinate. The surfaces $z = \pm d$ of the plate are assumed to be (i) stress free, isoconcentrated and thermally insulated/ isothermal or (ii) rigidly fixed, isoconcentrated and thermally insulated/ isothermal boundaries.

The basic governing equations for the displacement $\vec{u}(x,z,t) = (u,0,w)$, temperature change $T(x,z,t)$ and mass concentration $C(x,z,t)$ in the context of generalized thermo diffusion theory of solids, in the absence of body forces and heat sources are given by [8]

$$\mu\nabla^2\vec{u} + (\lambda+\mu)\nabla(\nabla\cdot\vec{u}) - \beta_1\nabla T - \beta_2\nabla C = \rho\ddot{\vec{u}}, \tag{2.1}$$

$$K\nabla^2 T - \rho C_e(\dot{T} + t_0\ddot{T}) - \beta_1 T_0\nabla\cdot(\dot{\vec{u}} + t_0\ddot{\vec{u}}) - aT_0(\dot{C} + t_0\ddot{C}) = 0, \tag{2.2}$$

$$\nabla^2 C - \frac{1}{Db}(\dot{C} + t_1\ddot{C}) - \frac{\beta_2}{b}T_0\nabla^2(\nabla\cdot\vec{u}) - \frac{a}{b}\nabla^2 T = 0, \tag{2.3}$$

where

$$\nabla = \Big(\frac{\partial}{\partial x}, 0, \frac{\partial}{\partial z}\Big), \qquad \nabla^2 = \frac{\partial^2}{\partial^2 x} + \frac{\partial^2}{\partial^2 z},$$
$$\beta_1 = (3\lambda+2\mu)\alpha_T, \qquad \beta_2 = (3\lambda+2\mu)\alpha_C,$$

α_T is coefficient of linear thermal expansion, α_C is coefficient of linear diffusion expansion, λ and μ are Lame's parameters, ρ is density, C_e is specific heat, a is thermodiffusive constant, b is diffusive constant, K is thermal conductivity, C is concentration, T is temperature change, t_0 and t_1 are thermal relaxation times.

Upon using Helmholtz representation for displacements through the relations

$$u = \frac{\partial\varphi}{\partial x} + \frac{\partial\psi}{\partial z}, \qquad w = \frac{\partial\varphi}{\partial z} - \frac{\partial\psi}{\partial x}, \tag{2.4}$$

in Eqs. (2.1)-(2.3), we obtain

$$\nabla^2\varphi - \ddot{\varphi} - \bar{\beta}C - T = 0, \tag{2.5}$$

$$\nabla^2\psi = \frac{\ddot{\psi}}{\delta^2}, \tag{2.6}$$

$$\nabla^2 T - (\dot{T} + t_0\ddot{T}) - \varepsilon_T\nabla^2(\dot{\varphi} + t_0\ddot{\varphi}) - \bar{a}(\dot{C} + t_0\ddot{C}) = 0, \tag{2.7}$$

$$\nabla^2 C - \varpi_b(\dot{C} + t_1\ddot{C}) - \nabla^4\varphi - \bar{b}\nabla^2 T = 0, \tag{2.8}$$

where we have introduced the quantities

$$x' = \frac{\omega^* x}{C_L}, \qquad z' = \frac{\omega^* z}{C_L}, \qquad t' = \omega^* t, \qquad u' = \frac{\rho\omega^* C_L u}{\beta_1 T_0}, \qquad w' = \frac{\rho\omega^* C_L w}{\beta_1 T_0}, \tag{2.9a}$$

$$T' = \frac{T}{T_0}, \qquad C' = \frac{C}{C_0}, \qquad t_0' = \omega^* t_0, \qquad t_1' = \omega^* t_1, \qquad \omega^* = \frac{C_e(\lambda + 2\mu)}{K}, \tag{2.9b}$$

$$\bar{a} = \frac{aC_0}{\rho C_e}, \qquad \bar{b} = \frac{aT_0}{bC_0}, \qquad \varpi_b = \frac{c_L^2}{\omega^* Db}, \qquad c_L^2 = \frac{\lambda + 2\mu}{\rho}, \qquad c_S^2 = \frac{\mu}{\rho} \tag{2.9c}$$

$$\delta^2 = \frac{c_S^2}{c_L^2}, \qquad \bar{\beta} = \frac{\beta_2 C_0}{\beta_1 T_0}, \qquad \varepsilon_T = \frac{T_0\beta_1^2}{\rho C_e(\lambda + 2\mu)}, \qquad \varepsilon_c = \frac{\beta_1\beta_2 T_0}{\rho C_e(\lambda + 2\mu)}. \tag{2.9d}$$

3 Boundary conditions

The following two sets of boundary conditions are assumed to be satisfied at the surfaces $z = \pm d$ of the plate:

$$\text{(i)} \qquad \sigma_{zz} = 0 = \sigma_{xz}, \qquad C = 0, \qquad \frac{\partial T}{\partial z} = 0 \quad (\text{or } T = 0), \tag{3.1}$$

$$\text{(ii)} \qquad u = 0 = w, \qquad C = 0, \qquad \frac{\partial T}{\partial z} = 0 \quad (\text{or } T = 0). \tag{3.2}$$

Here the stresses σ_{zz} and σ_{xz} can be written for the constitutive relations with the help of Eqs. (2.4)-(2.6) and quantities (2.9) as follows:

$$\sigma_{zz} = \ddot{\varphi} - 2\delta^2\Big(\frac{\partial^2\varphi}{\partial x^2} + \frac{\partial^2\psi}{\partial x\partial z}\Big), \qquad \sigma_{xz} = \ddot{\psi} + 2\delta^2\Big(\frac{\partial^2\varphi}{\partial x\partial z} - \frac{\partial^2\psi}{\partial x^2}\Big). \tag{3.3}$$

4 Solution of the problem

We take the solution of the form

$$(\varphi, \psi, C, T) = \big(\tilde{\varphi}(z), \tilde{\psi}(z), \tilde{C}(z), \tilde{T}(z)\big)\exp\{i\xi(x - ct)\}, \tag{4.1}$$

where $c = \omega/\xi$ is non-dimensional phase velocity, $\omega(\omega' = \omega/\omega^*)$ and $\xi(\xi' = \xi c_L/\omega^*)$ are the non-dimensional circular frequency and wave number, respectively. The primes have been suppressed for convenience.

Upon using solution (4.1) in Eqs. (2.5)-(2.8) and solving resulting system of equations, the expression for φ, ψ, T and C are obtained as

$$\varphi = \Big[\sum_{j=1}^{3} (A_J \sin m_j z + B_J \cos m_j z)\Big] \exp\{i\xi(x-ct)\}, \tag{4.2}$$

$$T = \Big[\sum_{j=1}^{3} S_j(A_j \sin m_j z + B_J \sin m_j z)\Big] \exp\{i\xi(x-ct)\}, \tag{4.3}$$

$$C = \Big[\sum_{j=1}^{3} V_j(A_J \sin m_j z + B_J \cos m_j z)\Big] \exp\{i\xi(x-ct)\}, \tag{4.4}$$

$$\psi = (A_4 \sin \beta z + B_4 \cos \beta z) \exp\{i\xi(x-ct)\}, \tag{4.5}$$

where

$$S_j = \frac{\xi^2 c^2 \Big\{(1-a_j^2)\Big[(1+\overline{\beta b})a_j^2 - \tau_1\overline{\omega}_b\Big] - \overline{\beta b} a_j^2\Big[1-(1+\varepsilon_a)a_j^2\Big]\Big\}}{(1+\overline{\beta b})a_j^2 - \tau_1\overline{\omega}_b},$$

$$V_j = \frac{\xi^2 c^2 \bar{b} a_j^2\Big[1-(1+\varepsilon_a)a_j^2\Big]}{(1+\overline{\beta b})a_j^2 - \tau_1\overline{\omega}_b}, \tag{4.6}$$

$$\beta^2 = \xi^2\Big(\frac{c^2}{\delta^2}-1\Big), \qquad \alpha^2 = \xi^2(c^2-1), \qquad \tau_0 = t_0 + i\omega^{-1},$$

$$\tau_1 = t_1 + i\omega^{-1}, \qquad m_j^2 = \xi^2(a_j^2 c^2 - 1), \qquad j = 1,2,3. \tag{4.7}$$

Here a_j^2 are roots of complex cubic equation

$$A^3 - LA^2 + MA - N = 0, \tag{4.8}$$

where

$$L = \frac{\Big\{1 + \tau_1\bar{\omega}_b + \tau_0\Big[(1+\overline{ab})(1+\varepsilon_a) + (1+\overline{\beta b})(\varepsilon_T - \varepsilon_a)\Big]\Big\}}{(1-\varepsilon_C\overline{\beta})}, \tag{4.9}$$

$$M = \frac{\tau_0(1+\overline{ab}) + \tau_1\bar{\omega}_b\Big[1+\tau_0(1+\varepsilon_T)\Big]}{(1-\varepsilon_C\overline{\beta})}, \tag{4.10}$$

$$N = \frac{\tau_0\tau_1\overline{\omega}_b}{(1-\varepsilon_C\overline{\beta})}. \tag{4.11}$$

The displacement components u and w can be obtained by using Eqs. (4.2)-(4.5) in (2.4) as

$$u = \Big[\sum_{j=1}^{3} i\xi(A_j \sin m_j z + B_j \cos m_j z) + \beta(A_4 \cos\beta z - B_4 \sin\beta z)\Big] \exp\{i\xi(x-ct)\}, \tag{4.12}$$

$$w = \Big[\sum_{j=1}^{3} m_j (A_j \cos m_j z - B_j \sin m_j z) - i\xi (A_4 \sin \beta z + B_4 \cos \beta z) \Big] \exp\{ i\xi (x - ct) \}. \tag{4.13}$$

5 Secular equations

In this section we derive the secular equations which govern the motion of a plate subjected to stress-free, isoconcentrated and thermally insulated/ isothermal and rigidly fixed, isoconcentrated and thermally insulated/ isothermal boundary conditions on its surfaces $z = \pm d$.

5.1 Stress-free boundaries

Invoking the boundary conditions (3.1) at the surfaces $z = \pm d$ of the plate and using Eqs. (4.2)-(4.5), we obtain the system of eight simultaneous linear equations in the unknowns $(A_1, A_2, A_3, A_4, B_1, B_2, B_3, B_4)^T$. This system of equations has a non-trivial solution if and only if the determinant of the coefficient of amplitudes vanishes. After applying lengthy algebraic reductions and simplifications, the secular equations for stress-free, isoconcentrated, isothermal and stress-free, isoconcentrated, thermally insulated boundaries of the plate are respectively, obtained as

$$\Big(\frac{\tan m_4 d}{\tan m_1 d}\Big)^{\pm 1} + X \Big(\frac{\tan m_4 d}{\tan m_2 d}\Big)^{\pm 1} + Y \Big(\frac{\tan m_4 d}{\tan m_3 d}\Big)^{\pm 1} = Z, \tag{5.1}$$

$$\begin{aligned} \Big(\frac{\tan m_1 d}{\tan m_4 d}\Big)^{\pm 1} + X' \Big(\frac{\tan m_2 d}{\tan m_4 d}\Big)^{\pm 1} + Y' \Big(\frac{\tan m_1 d}{\tan m_4 d}\Big)^{\pm 1} &= G' \Big[\Big(\frac{\tan m_1 d}{\tan m_4 d}\frac{\tan m_2 d}{\tan m_4 d}\Big)^{\pm 1} \\ &+ X'' \Big(\frac{\tan m_2 d}{\tan m_4 d}\frac{\tan m_3 d}{\tan m_4 d}\Big)^{\pm 1} + Y'' \Big(\frac{\tan m_3 d}{\tan m_4 d}\frac{\tan m_1 d}{\tan m_4 d}\Big)^{\pm 1} \Big], \end{aligned} \tag{5.2}$$

where

$$X = \frac{m_2 (V_3 S_1 - V_1 S_3)}{m_1 (V_2 S_3 - V_3 S_2)}, \qquad Y = \frac{m_3 (V_1 S_2 - V_2 S_1)}{m_1 (V_2 S_3 - V_3 S_2)}, \tag{5.3a}$$

$$X' = \frac{m_3 m_1 V_2 (S_3 - S_1)}{m_2 m_3 V_1 (S_2 - S_3)}, \qquad Y' = \frac{m_1 m_2 V_3 (S_1 - S_2)}{m_2 m_3 V_1 (S_2 - S_3)}, \tag{5.3b}$$

$$Z = -\frac{(\beta^2 - \xi^2)^2}{4\xi^2 \beta m_1 (V_2 S_3 - V_3 S_2)} \Big[V_1 (S_2 - S_3) + V_2 (S_3 - S_1) + V_3 (S_1 - S_2) \Big], \tag{5.3c}$$

$$G' = \frac{(\beta^2 - \xi^2)^2 m_1 S_1 (V_2 - V_3)}{4\xi^2 \beta m_2 m_3 V_1 (S_2 - S_3)}, \tag{5.3d}$$

$$X'' = \frac{m_1 S_1 (V_2 - V_3)}{m_1 S_1 (V_2 - V_3)}, \qquad Y'' = \frac{m_3 S_3 (V_1 - V_2)}{m_1 S_1 (V_2 - V_3)}. \tag{5.3e}$$

Here, the superscript -1 corresponds to symmetric and $+1$ refers to skew symmetric modes.

5.2 Rigidly fixed boundaries

By invoking boundary conditions (3.2) on the boundaries $z = \pm d$ of the plate, we again arrive at the system of eight simultaneous linear equations in amplitudes vector $(A_1, A_2, A_3, A_4, B_1, B_2, B_3, B_4)^T$. The condition of existence of non-trivial solution of this system leads to the secular equations in the case of rigidly fixed, isoconcentrated, isothermal and rigidly fixed, isoconcentrated, thermally insulated plates. These secular equations have the same form as that of Eqs. (5.1)-(5.2) except that the quantities Z and G' will get replaced with

$$Z^* = \frac{-\xi^2}{\beta m_1(V_2S_3 - V_3S_2)}\Big[V_1(S_2 - S_3) + V_2(S_3 - S_1) + V_3(S_1 - S_2)\Big], \tag{5.4a}$$

$$G^* = \frac{-\xi^2 m_1 S_1(V_2 - V_3)}{\beta m_2 m_3 V_1(S_2 - S_3)}. \tag{5.4b}$$

respectively.

6 Regions of secular equations

The close inspection reveals that the secular Eqs. (5.1)-(5.2) are complex transcendental equations, which contain complete information about various characteristics of the plate waves such as the phase velocity, wave number, attenuation coefficient, specific loss and relative frequency shift etc. Depending upon whether m_1, m_2, m_3, β are real, purely imaginary or complex, the frequency Eqs. (5.1)-(5.2) are correspondingly altered as follows:

Region I When the characteristic roots are of the type

$$\alpha^2 = -\alpha'^2, \quad \beta^2 = -\beta'^2, \quad m_j^2 = -m_j'^2, \quad j = 1, 2, 3,$$

so that

$$\alpha = -i\alpha', \quad \beta = -i\beta', \quad m_j = -im_j', \quad j = 1, 2, 3,$$

are purely imaginary or complex numbers. In this case the secular equations are written from Eqs. (5.1)-(5.2) by replacing circular tangent functions with hyperbolic tangent functions.

Region II If two of the characteristic roots are of the type

$$\alpha^2 = -\alpha'^2, \quad m_j^2 = -m_j'^2, \quad j = 1, 2, 3,$$

so that

$$\alpha = -i\alpha', \quad m_j = -im_j', \quad j = 1, 2, 3,$$

then the frequency equations can be obtained from Eqs. (5.1)-(5.2) by replacing circular tangent functions of m_j ($j = 1, 2, 3$) with hyperbolic tangent functions.

Region III In the general case, the characteristic roots are given by m_j^2 ($j = 1, 2, 3$), α^2, β^2, and the secular equations are given by Eqs. (5.1)-(5.2).

7 Solution of secular equations

In general, the wave number and hence the phase velocity of the waves is a complex quantity, therefore the waves are attenuated in space. If we write

$$c^{-1} = V^{-1} + i\omega^{-1}Q, \tag{7.1}$$

so that $\xi = R + iQ$, where $R = \omega/V$ and Q are real numbers. Here V is the propagation speed and Q the attenuation coefficient of the waves. Upon using representation (7.1) in secular Eq. (5.2), the values of propagation speed V and attenuation coefficient Q for different modes of wave propagation can be obtained. Since $c' = c/c_1$ is the non-dimensional complex phase velocity, so $V' = V/c_1$ and $Q' = c_1 Q$ are the non-dimensional phase speed and attenuation coefficient, respectively. Here dashes have been omitted for convenience.

Upon using representation (7.1) in secular Eqs. (5.1)-(5.2) which on separating the real and imaginary parts provide us

$$\frac{T_1}{T_4} + \frac{X_1 D_1}{D_2}\frac{T_2}{T_4} + \frac{Y_1 D_1}{D_3}\frac{T_3}{T_4} - \frac{Z_1 D_1}{D_4} = \frac{X_2 D_1}{D_2^*}\frac{T_2'}{T_4} + \frac{Y_2 D_1}{D_3^*}\frac{T_3'}{T_4} - \frac{Z_2 D_1}{D_4^*}\frac{T_4'}{T_4}, \tag{7.2}$$

$$\frac{T_1'}{T_4'} + \frac{X_1 D_1^*}{D_2^*}\frac{T_2'}{T_4'} + \frac{Y_1 D_1^*}{D_3^*}\frac{T_3'}{T_4'} - \frac{Z_1 D_1^*}{D_4^*} = -\frac{X_2 D_1^*}{D_2}\frac{T_2}{T_4'} - \frac{Y_2 D_1^*}{D_3}\frac{T_3}{T_4'} + \frac{Z_2 D_1^*}{D_4}\frac{T_4}{T_4'}, \tag{7.3}$$

$$\frac{T_1}{T_4} + \frac{X_1' D_1}{D_2}\frac{T_2}{T_4} + \frac{Y_1' D_1}{D_3}\frac{T_2}{T_4} - \Delta_1 = \frac{X_2' D_1}{D_2^*}\frac{T_2'}{T_4} + \frac{Y_2' D_1}{D_2^*}\frac{T_3'}{T_4} - \Delta_2 - \Delta_3, \tag{7.4}$$

$$\frac{T_1'}{T_4'} + \frac{X_1' D_1^*}{D_2^*}\frac{T_2'}{T_4'} + \frac{Y_1' D_1^*}{D_3^*}\frac{T_3'}{T_4'} - \Delta_4 = -\frac{X_2' D_1^*}{D_2}\frac{T_2}{T_4'} - \frac{Y_2' D_1^*}{D_3}\frac{T_3}{T_4'} - \Delta_5 + \Delta_6, \tag{7.5}$$

where $T_i = \tan(2p_i d)$, $T_i' = \tanh(2q_i d)$, $i = 1,2,3,4$;

$$(p_i, q_i) = \big(\mathrm{Re}(m_i), \mathrm{Im}(m_i)\big), \quad (i = 1,2,3), \qquad (p_4, q_4) = \big(\mathrm{Re}(\beta), \mathrm{Im}(\beta)\big), \tag{7.6a}$$

$$(X_1, X_2) = \big(\mathrm{Re}(X), \mathrm{Im}(X)\big), \qquad (Y_1, Y_2) = \big(\mathrm{Re}(Y), \mathrm{Im}(Y)\big), \tag{7.6b}$$

$$(X_1', X_2') = \big(\mathrm{Re}(X'), \mathrm{Im}(X')\big), \qquad (Y_1', Y_2') = \big(\mathrm{Re}(Y'), \mathrm{Im}(Y')\big), \tag{7.6c}$$

$$(X_1'', X_2'') = \big(\mathrm{Re}(X''), \mathrm{Im}(X'')\big), \qquad (Y_1'', Y_2'') = \big(\mathrm{Re}(Y''), \mathrm{Im}(Y'')\big), \tag{7.6d}$$

$$(Z_1, Z_2) = \big(\mathrm{Re}(Z), \mathrm{Im}(Z)\big), \qquad (G_1', G_2') = \big(\mathrm{Re}(G'), \mathrm{Im}(G')\big). \tag{7.6e}$$

$\Delta_i (i = 1,2,3,4,5,6)$ are given in Appendix.

$$D_i = \begin{cases} 1 + \frac{\cosh 2q_i d}{\cos 2p_i d}, & \text{for asymmetric,} \\ \frac{\cosh 2q_i d}{\cos 2p_i d} - 1, & \text{for asymmetric,} \end{cases} \tag{7.7a}$$

$$D_i^* = \begin{cases} 1 + \frac{\cos 2p_i d}{\cosh 2q_i d}, & \text{for asymmetric,} \\ \frac{\cos 2p_i d}{\cosh 2q_i d} - 1, & \text{for asymmetric,} \end{cases} \tag{7.7b}$$

$$D_4 = \begin{cases} 1 + \frac{\cosh 2q_4 h}{\cos 2p_4 h}, & \text{for asymmetric,} \\ \frac{\cosh 2q_4 h}{\cos 2p_4 h} - 1, & \text{for asymmetric,} \end{cases} \tag{7.7c}$$

$$D_4^* = \begin{cases} 1 + \frac{\cos 2p_4 h}{\cosh 2q_4 h}, & \text{for asymmetric,} \\ \frac{\cos 2p_4 h}{\cosh 2q_4 h} - 1, & \text{for asymmetric.} \end{cases} \tag{7.7d}$$

Upon using representation (7.1) the complex roots a_i^2 $(i = 1,2,3)$ of Eq. (4.6) are computed with the help of reduced Cardano's method. The characteristic roots a_i^2 $(i = 1,2,3)$ are further used to solve the secular Eqs. (5.1)-(5.2) to obtain phase velocity (V) and attenuation coefficient (Q) by using function iteration numerical technique outlined below [14].

The each of the real secular Eqs. (7.2)-(7.5) are $f(V,Q) = 0$ and $g(V,Q) = 0$. In order to apply functional iteration method we write $V = f^*(V,Q)$ and $Q = g^*(V,Q)$, where the functions f^* and g^* are selected in such a way that they satisfy the conditions

$$\Big|\frac{\partial f^*}{\partial V}\Big| + \Big|\frac{\partial f^*}{\partial Q}\Big| < 1, \qquad \Big|\frac{\partial g^*}{\partial V}\Big| + \Big|\frac{\partial g^*}{\partial Q}\Big| < 1, \tag{7.8}$$

for all V, Q in the neighbourhood of the root. If (V_0, Q_0) be the initial approximation to the root, then we construct the successive approximations according to the formulae

$$\begin{aligned} V_1 &= f^*(V_0,Q_0) \quad \cdots \quad Q_1 = g^*(V_1,Q_0), \\ V_2 &= f^*(V_1,Q_1) \quad \cdots \quad Q_2 = g^*(V_2,Q_1), \\ &\vdots \qquad\qquad\qquad \vdots \qquad\quad \vdots \\ V_{n+1} &= f^*(V_n,Q_n) \cdots \quad Q_{n+1} = g^*(V_{n+1},Q_n). \end{aligned} \tag{7.9}$$

The sequence $\{V_n, Q_n\}$ of approximations to the root will converge to the actual value (V_0, Q_0) of the root provided (V_0, Q_0) lies in the neighbourhood of the actual root. For the initial value $c = c_0 = (V_0, Q_0)$, the roots a_j $(j = 1,2,3)$ are computed from Eqs. (7.2)-(7.5) by using Cardano's procedure for each value of the wave number R, for an assigned frequency. The values of a_j $(j = 1,2,3)$ so obtained are then used in secular Eqs. (7.2)-(7.5) to obtain the current values of V and Q each time which are further used to generate the sequence (7.9). The process is terminated as and when the condition $|V_{n+1} - V_n| < \varepsilon$, ε being arbitrarily small number to be selected at random to achieve the accuracy level, is satisfied. The procedure is continuously repeated for different values of the wave number R to obtain corresponding values of the phase velocity (V) and attenuation coefficient (Q) We have selected tolerance $\varepsilon = 10^{-5}$ for the purpose of numerical computations in Section 10.

The specific loss factor being the measure of energy dissipation in a specimen through a stress cycle (ΔW) to the elastic energy (W) stored in the specimen at maximum strain is also computed. For a sinusoidal plane wave of small amplitude, Kolsky [15] shows that the specific loss $\Delta W/W$ equals 4π times the absolute value of the imaginary part of ξ to the real part of ξ. Hence

$$\Big|\frac{\Delta W}{W}\Big| = 4\pi\Big|\frac{\mathrm{Im}(\xi)}{\mathrm{Re}(\xi)}\Big| = 4\pi\Big|\frac{VQ}{\omega}\Big|. \tag{7.10}$$

The thermo-mechanical coupling factor (K^2) is defined as

$$K^2 = \left| \frac{V_{ins} - V_{iso}}{V_{iso}} \right|, \tag{7.11}$$

where V_{ins} and V_{iso} are the real phase speeds of the wave under thermally insulated and isothermal boundary conditions prevailing at the stress free surface of the material half space. The relative frequency shifts Ω_i ($i = 1, 2$), of acoustic symmetric and asymmetric modes are defined as:

$$\Omega_i = \left| \frac{\omega_{ins} - \omega_{iso}}{\omega_{iso}} \right|, \quad i = 1, 2. \tag{7.12}$$

8 Special cases of secular equations

In this section we discuss the reduction of secular equations in case of thin and thick plate structures.

8.1 Long-wavelength waves

In the case of thin plates the transverse wavelength with respect to thickness is quite large, so that $\xi d \ll 1$. The Regions I and II yield the results of interest in this case. In Region I, the symmetric case has no roots. For the skew-symmetric case, on retaining the first two terms in the expression of hyperbolic tangents, the secular Eq. (5.2) for stress-free, isoconcentrated and thermally insulated case reduces to

$$-(\xi^2 - \beta^2)^2 = \frac{d^2}{3} \Big[4\xi^2 \beta^4 + 4\xi^2 \beta^2 \frac{F^*}{F} + (\beta^2 + \xi^2)^2 \frac{G}{F} \Big], \tag{8.1}$$

where

$$\begin{aligned} F^* &= V_1(S_2 - S_3) + V_2(S_3 - S_1) + V_3(S_1 - S_2), \\ F &= m_1'^2 V_1(S_2 - S_3) + m_2'^2 V_2(S_3 - S_1) + m_3'^2 V_3(S_1 - S_2), \\ G &= (m_2'^2 + m_3'^2) S_1 (V_2 - V_3) + (m_3'^2 + m_1'^2) S_2 (V_3 - V_1) \\ &\quad + (m_1'^2 + m_2'^2) S_3 (V_1 - V_2). \end{aligned}$$

Thus on discarding the terms of higher order than $(c/\delta)^4$, we obtain

$$c = \frac{2\xi \delta d}{\sqrt{3}} \Big[1 + \delta^2 \Big(\frac{\bar{F} + \bar{G}}{\bar{F}^*} \Big) \Big]^{\frac{1}{2}}, \tag{8.2}$$

where

$$\bar{F}^* = \bar{V}_1(\bar{S}_2 - \bar{S}_3) + \bar{V}_2(\bar{S}_3 - \bar{S}_1) + \bar{V}_3(\bar{S}_1 - \bar{S}_2), \tag{8.3a}$$

$$\bar{F} = a_1^2 \bar{V}_1(\bar{S}_2 - \bar{S}_3) + a_2^2 \bar{V}_2(\bar{S}_3 - \bar{S}_1) + a_3^2 \bar{V}_3(\bar{S}_1 - \bar{S}_2), \tag{8.3b}$$

$$\bar{G} = (a_2^2 + a_3^2) \bar{S}_1 (\bar{V}_2 - \bar{V}_3) + (a_3^2 + a_1^2) \bar{S}_2 (\bar{V}_3 - \bar{V}_1) + (a_1^2 + a_2^2) \bar{S}_3 (\bar{V}_1 - \bar{V}_2), \tag{8.3c}$$

$$\bar{S}_j = 1 - a_j^2 - \overline{\beta V_j}, \qquad \bar{V}_j = \frac{\bar{b}a_j^2\Big[1 - (1+ \in_a)a_j^2\Big]}{1 + \overline{\beta \bar{b}}a_j^2 - \tau_1\bar{\omega}_b}, \qquad j = 1,2,3. \tag{8.3d}$$

Using representation (7.1) in Eq. (8.2) and on separating real and imaginary complex parts, we find that the real phase speed and attenuation coefficient of thin plate waves in this case given by

$$V = \frac{2R\delta d}{\sqrt{r}}\sqrt{\frac{1-\delta^2}{3}}\sec^2\frac{\theta}{4}, \qquad Q = R\tan\frac{\theta}{4}, \tag{8.4}$$

where

$$r = \sqrt{(1+\delta_R^*)^2 + (\delta_I^*)^2}, \qquad \theta = \tan^{-1}\Big(-\frac{\delta_I^*}{1+\delta_R^*}\Big), \tag{8.5a}$$

$$\delta^* = \frac{\delta^2}{1-\delta^2}\Big(1 + \frac{\bar{F}+\bar{G}}{\bar{F}^*}\Big), \quad \delta_R^* = \mathrm{Re}(\delta^*), \qquad \delta_I^* = \mathrm{Im}(\delta^*). \tag{8.5b}$$

In the absence of mass diffusion ($\bar{a} = 0 = \bar{\beta}$), the Eq. (8.4) reduces to

$$V = 2R\delta d\sqrt{\frac{1-\delta^2}{3}}, \qquad Q = 0.$$

This result with linear dependence of V on R agrees with the one derived from classical theory in elastokinetics (see Graff [16]) and of course pertains to the flexural vibrations and represents only a single vibration mode of limited frequency range in over all frequency spectrums.

In Region II, the skew-symmetric case has no roots. The secular Eq. (5.2) for symmetric case provides us with

$$\begin{aligned} &m_1'^2S_1(V_2-V_3) + m_2'^2S_2(V_3-V_1) + m_3'^2S_3(V_1-V_2) \\ =&-\frac{4\xi^2}{(\beta^2-\xi^2)^2}\left[m_2'^2m_3'^2V_1(S_2-S_3) + m_3'^2m_1'^2V_2(S_3-S_1)\right. \\ &\left. +m_1'^2m_2'^2V_3(S_1-S_2)\right]. \end{aligned} \tag{8.6}$$

The Eq. (8.3) on simplification reduces to a quadratic equation in c^2 and gives us two pairs of values of the complex phase velocity as

$$c_1 = \pm\lambda_1, \qquad c_2 = \pm\lambda_2, \tag{8.7}$$

where

$$\lambda_1^2,\ \lambda_2^2 = \frac{A_1 \pm \sqrt{A_1^2 - 4A_2}}{2}, \tag{8.8a}$$

$$A_1 = \frac{\sum(1+4\delta^2a_1^2)\bar{S}_1(\bar{V}_2-\bar{V}_3) + 4\delta^4\sum\bar{V}_1(\bar{S}_2-\bar{S}_3)a_2^2a_3^2}{\sum\bar{S}_1(\bar{V}_2-\bar{V}_3)a_1^2}, \tag{8.8b}$$

$$A_2 = \frac{4\delta^2\Big[\sum\bar{S}_1(\bar{V}_2-\bar{V}_3) + \delta^2\sum(\bar{V}_2\bar{S}_3 - \bar{V}_3\bar{S}_2)a_1^2\Big]}{\sum\bar{S}_1(\bar{V}_2-\bar{V}_3)a_1^2}. \tag{8.8c}$$

Each pair of values in Eq. (8.7) corresponds to incoming and outgoing wave at any point and instant of time.

Using representation (7.1) in Eq. (8.7) lead to real values of phase velocity and attenuation coefficient as given below:

$$V_i = \frac{1}{\mathrm{Re}(\frac{1}{\lambda_i})}, \qquad Q = \omega \,\mathrm{Im}\left(\frac{1}{\lambda_i}\right), \quad i = 1, 2. \tag{8.9}$$

The results in the case of coupled thermo diffusive waves can be derived from (8.9) by setting $t_0 = 0 = t_1$. In the absence of mass diffusion ($\bar{a} = 0 = \bar{\beta}$), from (8.5) and (8.6) we have

$$A_1 = \frac{1 + 4\delta^2\tau_0(1 + \varepsilon_T - \delta^2)}{\tau_0(1 + \varepsilon_T)}, \qquad A_2 = \frac{4\delta^2(1 - \delta^2)}{\tau_0(1 + \varepsilon_T)}. \tag{8.10}$$

In the case of uncoupled theory of thermo elasticity (UCT), thermomechanical coupling parameter vanishes ($\varepsilon_T = 0$) and consequently for non-Fourier solid, we obtain

$$V_1 = 2\delta\sqrt{1 - \delta^2}, \qquad Q_1 = 0, \tag{8.11a}$$

$$V_2 = \frac{1}{\sqrt{r_1}} \sec\frac{\theta_1}{2}, \qquad Q_2 = \omega\sqrt{r} \sin\frac{\theta_1}{2}, \tag{8.11b}$$

where

$$r_1 = \frac{\sqrt{1 + \tau_0^2\omega^2}}{\omega}, \qquad \theta_1 = \tan^{-1}\left(\frac{1}{\tau_0\omega}\right).$$

In case heat conduction process follows Fourier's law ($t_0 = 0$), the phase velocity (V_1) and attenuation coefficient (Q_1) remains unaltered whereas V_2 and Q_2 are given by

$$V_2 = \sqrt{2\omega}, \qquad Q_2 = \sqrt{\frac{\omega}{2}}. \tag{8.12}$$

8.2 Short-wavelength waves

Let us consider the case when the transverse wavelength with respect to thickness is quite small, so that $\xi d \gg 1$. In this case the characteristic roots lie in Region I and some information on asymptotic behavior is obtainable by putting $\xi \to \infty$. For

$$\xi \to \infty, \qquad \frac{\tanh(m_j' d)}{\tanh(\beta_j d)} \to 1, \qquad j = 1, 2, 3,$$

the frequency Eqs. (5.1) and (5.2), respectively reduce to

$$m_1'(V_2S_3 - V_3S_2) + m_2'(V_3S_1 - V_1S_3) + m_3'(V_1S_2 - V_2S_1)$$

$$
\begin{aligned}
&=\frac{(\beta'^2+\xi^2)^2}{4\xi^2\beta'}\Big[V_1(S_2-S_3)+V_2(S_3-S_1)+V_3(S_1-S_2)\Big], && (8.13)\\
&m_2'm_3'V_1(S_2-S_3)+m_3'm_1'V_2(S_3-S_1)+m_1'm_2'V_3(S_1-S_2)\\
&=-\frac{(\beta'^2+\xi^2)^2}{4\xi^2\beta'}\Big[m_1'S_1(V_2-V_3)+m_2'S_2(V_3-V_1)+m_3'S_3(V_1-V_2)\Big]. && (8.14)
\end{aligned}
$$

These are the secular equations which govern the propagation of Rayleigh type surface waves in a thick plate. Because the thick plate under such conditions behaves like a half space and hence the transmission propagation of energy takes place mainly along the surface. Eqs. (8.13) and (8.14) are the same as obtained by Sharma et al. [13] and discussed in detail there in.

9 Displacement, temperature and concentration fields

The amplitudes of displacements, temperature and mass concentration for symmetric and skew-symmetric modes of the plate waves have also been computed for stress-free, thermo diffusive elastic plate under the propagation conditions of the considered modes of wave propagation.

$$
\begin{aligned}
(u)_{sy}=&\Big[i\xi(\cos m_1z+L_1\cos m_2z+L_2\cos m_3z)\\
&+\beta L_3\cos\beta z\Big]B_1\exp\Big\{i\xi(x-ct)\Big\}, && (9.1)\\
(u)_{asy}=&\Big[i\xi(\sin m_1z+M_1\sin m_2z+M_2\sin m_3z)\\
&-\beta M_3\sin\beta z\Big]A_1\exp\Big\{i\xi(x-ct)\Big\}, && (9.2)\\
(w)_{sy}=&-\Big[(m_1\sin m_1z+m_2L_1\sin m_2z+m_3L_2\sin m_3z)\\
&+i\xi L_3\sin\beta z\Big]B_1\exp\Big\{i\xi(x-ct)\Big\}, && (9.3)\\
(w)_{asy}=&\Big[(m_1\cos m_1z+m_2M_1\cos m_2z+m_3M_2\cos m_3z)\\
&-i\xi M_3\cos\beta z\Big]A_1\exp\Big\{i\xi(x-ct)\Big\}, && (9.4)\\
(T)_{sy}=&(S_1\cos m_1z+S_2L_1\cos m_2z+S_3L_2\cos m_3z)B_1\exp\Big\{i\xi(x-ct)\Big\}, && (9.5)\\
(T)_{asy}=&(S_1\sin m_1z+S_2M_1\sin m_2z+S_3M_2\sin m_3z)A_1\exp\Big\{i\xi(x-ct)\Big\}, && (9.6)\\
(C)_{sy}=&(V_1\cos m_1z+V_2L_1\cos m_2z+V_3L_2\cos m_3z)B_1\exp\Big\{i\xi(x-ct)\Big\}, && (9.7)\\
(C)_{asy}=&(V_1\sin m_1z+V_2M_1\sin m_2z+V_3M_2\sin m_3z)A_1\exp\Big\{i\xi(x-ct)\Big\}, && (9.8)
\end{aligned}
$$

where L_i, M_i $(i=1,2,3)$ are given in Appendix.

10 Numerical result and discussion

In order to illustrate and verify the analytical results obtained in the previous sections, we present some numerical simulation results. The material chosen for this purpose is brass $\left[copper(70\%)\ and\ zinc(30\%)\right]$, whose physical data is given below [9,17,18]:

$$
\begin{aligned}
&\lambda = 7.69\times 10^{10}Nm^{-2}, && \rho = 8.522\times 10^{3}Kgm^{-3},\\
&\mu = 3.62\times 10^{10}Nm^{-2}, && T_0 = 293^0K,\\
&\alpha_c = 1.8\times 10^{-5}K^{-1}, && D = 0.24\times 10^{-4}ms^{-1}(Zn-Cu),\\
&\alpha_T = 2.0\times 10^{-6}K^{-1}, && C_e = 385J/Kg/^0K,\\
&K = 1.11\times 10^{10}W/m^0K, && a = 0.1521\times 10^{2}ms^{-1},\\
&\beta_1 = 60.62\times 10^{4}Nm^{-2}K^{-1}, && b = 0.02\times 10^{4}ms^{-1},\\
&\beta_2 = 54.56\times 10^{5}Nm^{-5}K^{-1}, && \in_T = 0.0002198,\\
&\omega^* = 5.178\times 10^{11}s^{-1}.
\end{aligned}
$$

The value of thermal relaxation time t_0 is estimated from the relation $t_0 = 3K/\rho C_e c_L$ (see Chandrasekharaiah [19]) and that of t_1 is taken proportional to that of t_0. The secular Eqs. (7.2)-(7.5) have been solved numerically by employing the procedure described in Section 7 above to compute phase velocity, attenuation coefficient, specific loss factor of energy dissipation and relative frequency shift to explore the effect of various interacting fields and coupling parameters on these wave characteristics. The FORTRAN code has been developed for computer simulations and the sequence of iteration is allowed to iterate for sufficient number of times in order to achieve desired level of accuracy viz. four decimal places here. An infinite number of roots exist for a given value of frequency, which can be obtained by giving a value of wave number, from the secular equations. Note that case must be taken in the root finding procedure,

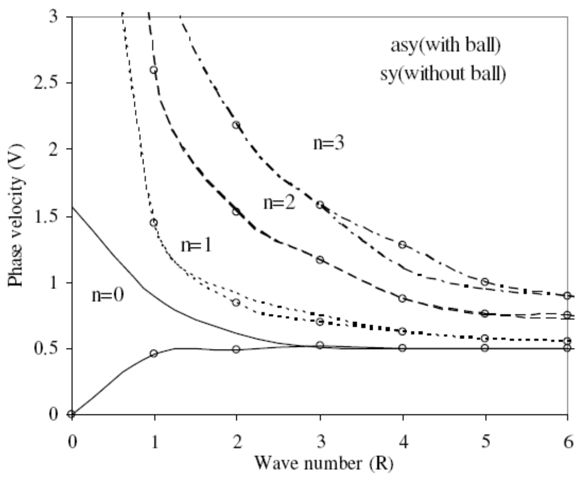

Figure 2: Phase velocity versus wave number for stress free, isoconcentrated and thermally insulated boundary.

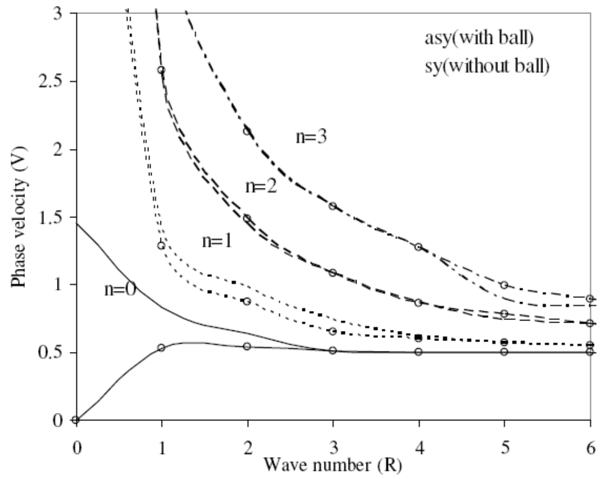

Figure 3: Phase velocity versus wave number for stress free, isoconcentrated and isothermal boundary.

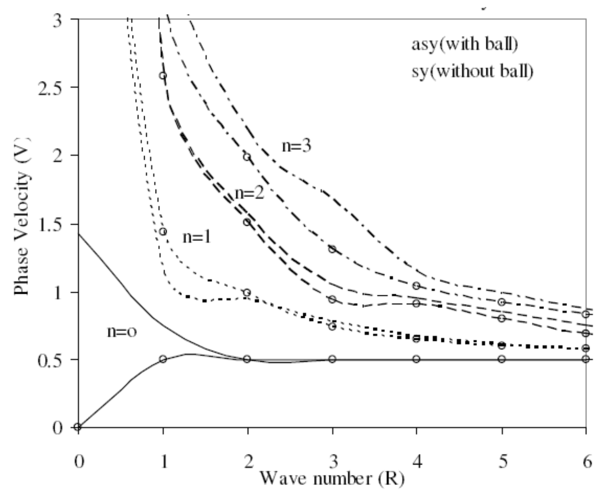

Figure 4: Phase velocity versus wave number for rigidly fixed isoconcentrated and isothermal boundary.

for the transcendental functions change their values rapidly. The computer simulated results have been presented in Figs. 2-8.

From Figs. 2 and 10 it is observed that the phase velocity of lowest (acoustic) asymmetric mode increases from a zero value at vanishing wave number in the range $0 \leq R \leq 3$ before it becomes steady and non-dispersive for $R \geq 3$. The phase velocity of acoustic symmetric mode decreases from a value greater than unity in the wave number range $0 \leq R \leq 3$ and almost varies linearly for $R \geq 3$. Figs. 4 and 5 reveal that the phase velocity profiles of acoustic modes, both asymmetric and symmetric, are subjected to dispersion in the wave number range $0 \leq R \leq 2$ in case of rigidly fixed plate in contrast to stress free plate in which case the effective range is

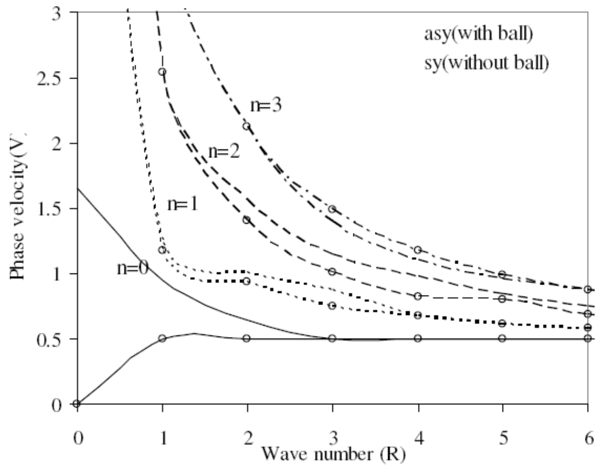

Figure 5: Phase velocity versus wave number for rigidly fixed isoconcentrated and thermally insulated boundary.

$0 \leq R \leq 3$. Beyond $R \geq 2$ the profiles of phase velocity becomes stable and steady with their asymptotic convergence to surface wave velocity under prevailing boundary conditions. It is pertinent to mention here that the phase velocity profiles of acoustic modes are subjected to significant dispersion at long wave lengths and ultimately become non-dispersive at short wave lengths with asymptotic convergence to elasto-thermodiffusive Rayleigh wave velocity. This is attributed to the fact that long wave length waves have deep penetrating capacity into the medium thereby creating significant disturbance in it due to which coupling between various interacting fields becomes operative. However, the short-wave length waves closely follow the surface as a wave guide without causing much disturbance to the plate which behaves like a half-space under such situations. The free surfaces admit a Rayleigh-type surface wave with complex wave number and hence phase velocity. Consequently, the surface wave propagates with attenuation due to the radiation of the energy from the surroundings into the medium. This radiated energy will be reflected back to the center of the plate by lower and upper surfaces. Thus the attenuated surface wave on the free surface is enhanced by this reflected energy to form a propagation wave. In fact, the multiple reflections between the upper and lower surfaces of the plate form caustics at one of the free surfaces and a strong stress concentration arises due to which the wave field becomes unbounded in the limit $d \to \infty$. The unbounded displacement field is characterized by the singularities of hyperbolic/ circular tangent functions.

It is also observed that as the thickness of the plate increases, the phase velocity decreases. This can be explained by the fact that as the thickness of the plate increases, the coupling effect of various interacting fields also increases, resulting in lower phase velocity. It can also be observed that the Rayleigh wave velocity is reached at lower wave number as the thickness increases, because the transportation of energy mainly takes place in the neighbourhood of the free surfaces of the thick plate in this case.

The phase velocity of higher (optical) modes of wave propagation, symmetric and asymmetric, attains quite large values at vanishing wave number, which decreases to become asymptotically close to the elastodiffusive shear wave velocity in all of Figs. 2-5. The magnitudes of phase velocities of optical symmetric and asymmetric, modes ($n > 1$) are observed to be developed at a rate of approximately n times the magnitude of the phase velocity of first harmonic ($n = 1$).

The phase velocity profiles of different optical modes, symmetric and asymmetric, behave identically for all values of the wave number except in case of $n = 1$ for $1.5 \leq R \leq 3.5$ and in the range $3 \leq R \leq 5.5$, $n = 3$ where these are subjected to some departure in stress free thermally insulated plate. However, this departure in the phase velocity profiles of symmetric and asymmetric modes occur in the wave number ranges $1 \leq R \leq 4$ and $4 \leq R \leq 6$ for the modes $n = 1$ and $n = 3$ respectively. The effect of different physical and mathematical conditions satisfied by mechanical, thermal or mass concentration fields at the surfaces of the plate is clearly visible from plots of Figs. 2-5. The profiles of various Lamb modes are subjected to many sign reversal throughout the thickness of the plate. The different optical modes appear at different cut-off frequencies with their increasing order as can be seen from the plots in these figures.

Fig. 6 represents the profiles of attenuation coefficient of acoustic modes with wave number in case of stress free, isoconcentrated and thermally insulated/ isothermal surfaces of the plate. It is noticed that the profiles of attenuation coefficient have a monotonic increase from zero value at vanishing wave number, in the wave number range $0 \leq R \leq 1$, to attain their maximum values at $R = 1$, before these start decreasing monotonically for $R \geq 1$ in order to vanish at extremely high wave numbers. It is also observed that equilibrium of heat flux at the surfaces of the plate results in more

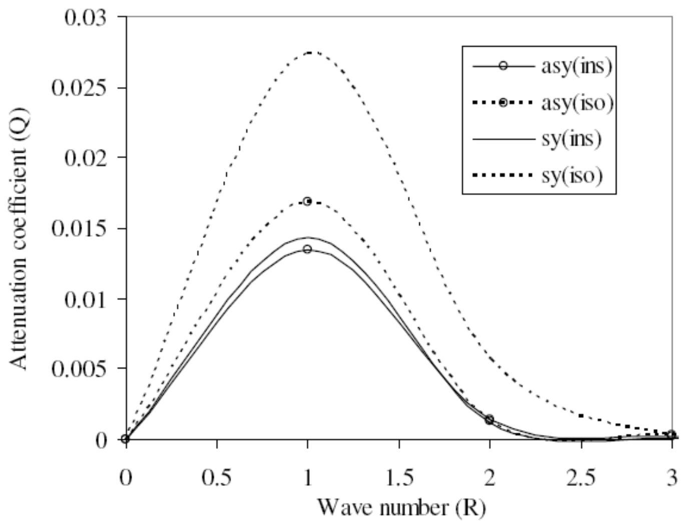

Figure 6: Attenuation of acoustic mode versus wave number for stress free boundary.

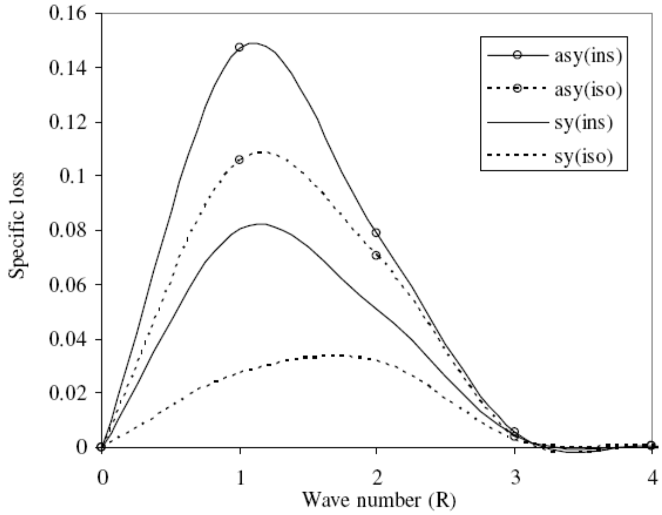

Figure 7: Specific loss factor of acoustic mode versus wave number for stress free boundary.

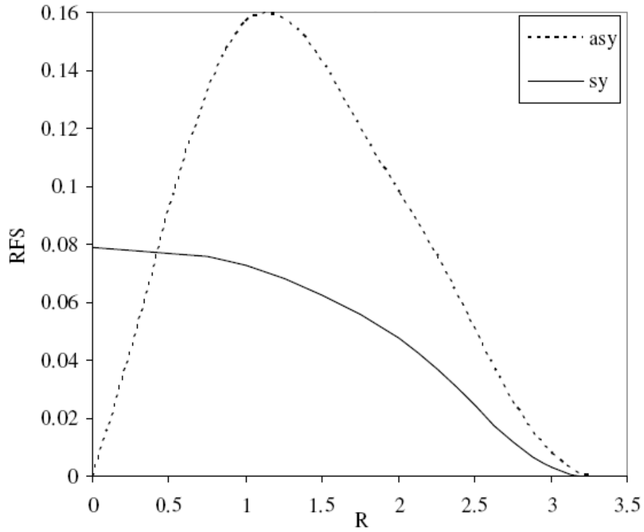

Figure 8: Relative frequency shift versus wave number for stress free boundary.

attenuation of the waves than that when the flow of heat flux is prevented across the surfaces of the plate. Moreover, symmetric modes are subjected to large attenuations as compared to asymmetric one in both the considered cases of boundary conditions.

Fig. 7 shows the variation of specific loss factor of energy dissipation, a measure of internal friction of the material, of acoustic modes with wave number in the case of stress free, isoconcentrated and thermally insulated/ isothermal surfaces of the plate. The specific loss factor of symmetric and asymmetric modes increases in the wave number range $0 \leq R \leq 1.2$ from zero value at vanishing wave number. The energy dissipation for asymmetric modes is more than that of symmetric modes in both the considered cases of boundary conditions. It is also noted that in case thermal equilibrium is prevailing at the surfaces of the plate, the energy dissipation is quite small as compared to that when the heat flux is prevented across the surfaces of the plate.

In Fig. 8 the respective relative frequency shifts (Ω_1) and (Ω_2) of acoustic symmetric and asymmetric modes respectively have been plotted versus wave number. The profile of relative frequency shift (Ω_1) decreases monotonically in the wave number range $0 \leq R \leq 3.2$ while that of (Ω_2) increases in the wave number range $0 \leq R \leq 1.2$ from zero value at vanishing wave number, decreases monotonically for $1.2 \leq R \leq 3.2$ and it vanishes afterwards.

11 Conclusions

Mass diffusion leads to significant attenuation in thin plate waves in Region I, while both mass concentration and thermal fields contribute to produce attenuating mechanical and thermal waves in Region II. However, the mechanical wave becomes non-attenuating in the absence of these fields but the thermal wave is still attenuating and becomes diffusive in the absence of thermal relaxation at high frequencies. At short wave lengths, the various modes of wave propagation closely follow Rayleigh surface wave motion. Thermal equilibrium at the surfaces of the plate results in more attenuation of acoustic mode of vibrations than that when the heat flux is prevented across the stress-free isoconcentrated surfaces of plate. Moreover, symmetric modes are subjected to large attenuations as compared to asymmetric one in both the considered cases of boundary conditions. However, the above trend will get reversed in the case of specific loss factor of energy dissipation.

Appendix

The quantities Δ_i $(i = 1,2,3,4,5,6)$ used in Eqs. (7.2)-(7.5) are defined as

$$
\begin{aligned}
\Delta_1 &= \frac{G_1' D_1}{D_2}\frac{T_1 T_2}{T_4^2} + \frac{(G_1' X_1'' - G_2' X_2'') D_1 D_4}{D_2 D_3}\frac{T_2 T_3}{T_4^2} + \frac{(G_1' Y_1'' - G_2' Y_2'') D_4}{D_3}\frac{T_3 T_1}{T_4^2}, \\
\Delta_2 &= G_2'\Big(\frac{D_4}{D_2^*}\frac{T_1 T_2'}{T_4^2} + \frac{D_1 D_4}{D_2 D_1^*}\frac{T_2 T_1'}{T_4^2}\Big) + (G_1' X_2'' + G_2' X_1'')\Big(\frac{D_1 D_4}{D_2 D_2^*}\frac{T_2 T_3'}{T_4^2} + \frac{D_1 D_4}{D_3 D_2^*}\frac{T_3 T_2'}{T_4^2}\Big) \\
&\quad + (G_1' Y_2'' + G_2' Y_1'')\Big(\frac{D_1 D_4}{D_3 D_1^*}\frac{T_3 T_1'}{T_4^2} + \frac{D_1 D_4}{D_1 D_3^*}\frac{T_1 T_3'}{T_4^2}\Big) - \frac{D_1 D_4}{D_4^*}\Big(\frac{X_2'}{D_2}\frac{T_2 T_4'}{T_4^2} + \frac{Y_2'}{D_3}\frac{T_3 T_4'}{T_4^2}\Big), \\
\Delta_3 &= \frac{G_1' D_1 D_4}{D_1^* D_2^*}\frac{T_1' T_2'}{T_4^2} + \frac{(G_1' Y_1'' - G_2' Y_2'') D_1 D_4}{D_1^* D_3^*}\frac{T_1' T_3'}{T_4^2} - \frac{D_1 D_4}{D_1^* D_4^*}\frac{T_1' T_4'}{T_4^2} \\
&\qquad + \frac{(G_1' X_1'' - G_2' X_2'') D_1 D_4}{D_2^* D_3^*}\frac{T_2' T_3'}{T_4^2} - \frac{X_1' D_1 D_4}{D_2^* D_4^*}\frac{T_2' T_4'}{T_4^2} - \frac{Y_1' D_1 D_4}{D_3^* D_4^*}\frac{T_3' T_4'}{T_4^2},
\end{aligned}
$$

$$\begin{aligned}
\Delta_4 =& \frac{X_2' D_4 D_1^*}{D_2^* D_4^*}\frac{T_2'}{T_4} + \frac{Y_2' D_4 D_1^*}{D_3^* D_4^*}\frac{T_3'}{T_4} - \frac{G_2' D_4}{D_2^*}\frac{T_1' T_2'}{T_4 T_4'} - \frac{(G_1' X_2'' + G_2' X_1'')D_4}{D_2^* D_3^*}\frac{T_2' T_3'}{T_4 T_4'} \\
&- \frac{(G_1' Y_2'' + G_2' Y_1'')D_4}{D_3^*}\frac{T_1' T_3'}{T_4 T_4'}, \\
\Delta_5 =& \frac{D_4 D_1^*}{D_1 D_4^*}\frac{T_1}{T_4} + \frac{X_1' D_4 D_1^*}{D_2 D_4^*}\frac{T_2}{T_4} + \frac{Y_1' D_4 D_1^*}{D_3 D_4^*}\frac{T_3}{T_4} - \frac{G_2' D_4 D_1^*}{D_1 D_2}\frac{T_1 T_2}{T_4 T_4'} \\
&- \frac{(G_1' X_2'' + G_2' X_1'')D_4 D_1^*}{D_2 D_3}\frac{T_2 T_3}{T_4 T_4'} - \frac{(G_1' Y_2'' + G_2' Y_1'')D_4 D_1^*}{D_1 D_3}\frac{T_1 T_3}{T_4 T_4'}, \\
\Delta_6 =& G_1'\Big(\frac{D_4 D_1^*}{D_1 D_2^*}\frac{T_1 T_2'}{T_4 T_4'} + \frac{D_4}{D_2}\frac{T_2 T_1'}{T_4 T_4'}\Big) + (G_1' X_2'' - G_2' X_1'')\Big(\frac{D_4 D_1^*}{D_2 D_3^*}\frac{T_2 T_3'}{T_4 T_4'} + \frac{D_4 D_1^*}{D_3 D_2^*}\frac{T_3 T_2'}{T_4 T_4'}\Big) \\
&+ (G_1' Y_2'' - G_2' Y_1'')\Big(\frac{D_4}{D_3}\frac{T_3 T_1'}{T_4 T_4'} + \frac{D_4 D_1^*}{D_1 D_3^*}\frac{T_1 T_3'}{T_4 T_4'}\Big).
\end{aligned}$$

The coefficients L_i, M_i ($i = 1,2,3$) used in Eqs. (9.1)-(9.4) are defined as

$$\begin{aligned}
L_1 =& \frac{\Big[(\beta^2-\xi^2)^2 T_4^*(V_3-V_1) - 4\beta\xi^2(m_3 V_1 T_3^* - m_1 V_3 T_1^*)\Big]c_1}{\Big[(\beta^2-\xi^2)^2 T_4^*(V_2-V_3) - 4\beta\xi^2(m_2 V_3 T_2^* - m_3 V_2 T_3^*)\Big]c_2}, \\
L_2 =& \frac{\Big[(\beta^2-\xi^2)^2 T_4^*(V_1-V_2) - 4\beta\xi^2(m_1 V_2 T_1^* - m_2 V_1 T_2^*)\Big]c_1}{\Big[(\beta^2-\xi^2)^2 T_4^*(V_2-V_3) - 4\beta\xi^2(m_2 V_3 T_2^* - m_3 V_2 T_3^*)\Big]c_3}, \\
L_3 =& \frac{2i\xi(\beta^2-\xi^2)\Big[(m_1 T_1^* - m_2 T_2^*)(V_3-V_1) - (m_3 T_3^* - m_1 T_1^*)(V_1-V_2)\Big]c_1}{\Big[(\beta^2-\xi^2)^2 T_4^*(V_2-V_3) - 4\beta\xi^2(m_2 V_3 T_2^* - m_3 V_2 T_3^*)\Big]c_4}, \\
M_1 =& \frac{\Big\{(\beta^2-\xi^2)^2 (T_4^*)^{-1}(V_3-V_1) - 4\beta\xi^2\Big[m_3 V_1 (T_3^*)^{-1} - m_1 V_3 (T_1^*)^{-1}\Big]\Big\}s_1}{\Big\{(\beta^2-\xi^2)^2 (T_4^*)^{-1}(V_2-V_3) - 4\beta\xi^2\Big[m_2 V_3 (T_2^*)^{-1} - m_3 V_2 (T_3^*)^{-1}\Big]\Big\}s_2}, \\
M_2 =& \frac{\Big\{(\beta^2-\xi^2)^2 (T_4^*)^{-1}(V_1-V_2) - 4\beta\xi^2\Big[m_1 V_2 (T_1^*)^{-1} - m_2 V_1 (T_2^*)^{-1}\Big]\Big\}s_1}{\Big\{(\beta^2-\xi^2)^2 (T_4^*)^{-1}(V_2-V_3) - 4\beta\xi^2\Big[m_2 V_3 (T_2^*)^{-1} - m_3 V_2 (T_3^*)^{-1}\Big]\Big\}s_3}, \\
M_3 =& \frac{-2i\xi(\beta^2-\xi^2)s_1(V_3-V_1)\Big[m_1 (T_1^*)^{-1} - m_2 (T_2^*)^{-1}\Big]}{\big\{(\beta^2-\xi^2)^2 (T_4^*)^{-1}(V_2-V_3) - 4\beta\xi^2\,\big[m_2 V_3 (T_2^*)^{-1} - m_3 V_2 (T_3^*)^{-1}\big]\big\}s_4} \\
&+ \frac{2i\xi(\beta^2-\xi^2)s_1(V_1-V_2)\Big[m_3 (T_3^*)^{-1} - m_1 (T_1^*)^{-1}\Big]}{\big\{(\beta^2-\xi^2)^2 (T_4^*)^{-1}(V_2-V_3) - 4\beta\xi^2\,\big[m_2 V_3 (T_2^*)^{-1} - m_3 V_2 (T_3^*)^{-1}\big]\big\}s_4},
\end{aligned}$$

where

$$\begin{aligned}
&c_j = \cos m_j d, \qquad s_j = \sin m_j d, \qquad T_j^* = \tan m_j d, \qquad j = 1,2,3, \\
&c_4 = \cos\beta d, \qquad s_4 = \sin\beta d, \qquad T_4^* = \tan\beta d.
\end{aligned}$$

Acknowledgments

The authors are thankful to the reviewers for their deep interest in this work and making useful suggestions for the improvement of this work.

References

[1] V. KOZIOV, *Thermoelastic vibrations of rectangular plates*, Prikl. Mekh. Tekhn. Fiz., 8 (1972), pp. 123–127.

[2] C. MASSALAS, A. DALAMANGAS AND A. LEONDITSIS, *Symmetric non-linear response of a circular plate due to heat flux at* $z = h/2$, Review of Romanian Science, Technology and Mechanical Applications, 28 (1983), pp. 643–650.

[3] H. S. SEXENA AND R. S. DHALIWAL, *Eigenvalue approach of coupled thermoelasticity*, J. Therm. Stresses., 13 (1990), pp. 161–175.

[4] A. B. KUMAR, *Thermoelastic waves from suddenly punched hole in a stretched plate*, Indian. J. Pure. Ap. Mat., 20 (1989), pp. 181–188.

[5] J. N. SHARMA, D. SINGH AND R. KUMAR, *Generalized thermoelastic waves in homogenous isotropic plates*, J. Acoust. Soc. Am., 108 (2000), pp. 848–851.

[6] J. N. SHARMA, *On the propagation of thermoelastic waves in homogenous isotropic plates*, Indian. J. Pure. Ap. Mat., 3 (2000), pp. 1329–1341.

[7] J. JIN, S. T. QUEK AND Q. WANG, *Wave boundary element to study lamb wave propagation in plates*, J. Sound. Vib., 288 (2005), pp. 195–213.

[8] H. H. SHERIEF, F. HAMZA AND H. SALEH, *The theory of generalized thermoelastic diffusion*, Int. J. Eng. Sci., 42 (2004), pp. 591–608.

[9] H. H. SHERIEF AND H. SALEH, *A half space problem in the theory of generalized thermoelastic diffusion*, Int. J. Solids. Struct., 42 (2005), pp. 4484–4493.

[10] M. AOUDI, *A generalized thermoelastic diffusion problem for an infinite long cylinder*, Int. J. of Math. Math. Sci., (2006), pp. 1–15.

[11] M. AOUDI, *Variable electrical and thermal conductivity in the theory of generalized thermoelastic diffusion*, Z. Angew. Math. Phys., 52(2) (2006), pp. 350–366.

[12] J. N. SHARMA, *Generalized thermoelastic diffusive waves in heat conducting materials*, J. Sound. Vib., 301 (2007), pp. 979–993.

[13] J. N. SHARMA, Y. D. SHARMA AND P. K. SHARMA, *On the propagation of elasto-thermodiffusive surface waves in heat conducting materials*, J. Sound. Vib., 315 (2008), pp. 927–938.

[14] J. N. SHARMA, Numerical Methods for Engineers and Scientists, Alpha Science International Ltd. Oxford, U. K., Second Edition, 2007.

[15] H. KOLSKY, Stress Waves in Solids, Dover Press New York, 1963.

[16] K. F. GRAFF, Wave Motion in Elastic Solids, Dover, New York, 1991.

[17] W. D. CALLISTER JR, Material Science and Engineering An Introduction, 6th edition Wiley India Private Limited, New Delhi, 2006.

[18] L. C. THOMS, Heat Transfer, Prentice Hall, Inc New Jersey, 1993.

[19] D. S. CHANDERASHEKHARIAH, *Thermoelasticity with second sound: A Review*, Appl. Mech. Rev., 39 (1986), pp. 355–376.